Inorg. Chem. **2006**, *45*, 5167−5171

Unusual In_2N_4 Cores in Complexes Containing Triazole-Based Chalcogen−Phosphoranyl Ligands

Mónica Moya-Cabrera,*,† Vojtech Jancik,† Rafael A. Castro,† Regine Herbst-Irmer,‡ and Herbert W. Roesky‡

Institute of Chemistry, UNAM, Circuito Exterior, Ciudad Universitaria, 04510, México, and Institute of Inorganic Chemistry, Georg-August Universität, Tammannstrasse 4, 37077, Göttingen, Germany

Received September 13, 2005

The 4,5-bis(diphenylphosphoranyl)-1,2,3-triazole [4,5-$(P(E)Ph_2)_2$tz] derivatives of indium $\{\kappa^3$-*N,N′,E*-[4,5-$(P(E)Ph_2)_2$-(μ−tz)]$InMe_2\}_2$ (E = O(**2**), S(**3**), Se(**4**)) were prepared in good yield. In addition, compound **5** (E = O, E′ = Se) was obtained from **4** through the replacement of a selenium atom in the P−Se(In) moiety by an oxygen atom, giving the mixed-chalcogen complex. The crystal structures of **2** and **5** exhibit a central $C_4In_2N_6O_2P_4$ core with an almost planar arrangement (mean deviation = 0.019 and 0.042 Å for **2** and 0.100 Å for **5**), while the $C_4In_2N_6S_2P_4$ core in **3** is nonplanar (mean deviation = 0.223 Å).

Introduction

During the past three decades, P−Y−P-unit-containing species (Y = N, C, alkyl, heterocycle) have received considerable attention as ligands in the coordination chemistry of p-block elements.[1] The Lewis base character of P(III) and its facile oxidation with elemental chalcogens or azides to P(V) modifies its coordination properties. In addition, the large variety of available Y linkage groups leads to further coordination diversity for these types of ligands.

Recently, Trofimenko reported the preparation of the 4,5-bis(diphenylphosphoranyl)-1,2,3-triazole [4,5-$(P(O)Ph_2)_2$tz] ligand and its complexes with uranium and cobalt, both of which display an interesting coordination behavior.[2] The uranium atom coordinates exclusively to the oxygen atoms, forming a seven-membered ring (UOPCCPO), while the Co is attached to one O and one N atom, forming a CoOPCN five-membered ring. The latter coordination pattern was also observed in palladium complexes containing the [4,5-$(P(S)Ph_2)_2$tz] ligand.[3] Motivated by an interest in the effects of these ligands on the coordination geometry of p-block elements, namely group 13 elements, we began a systematic study for indium compounds. Moreover, taking into account that group 13 elements form M_2N_4 six-membered rings with azoles,[4] multidentate ligands containing P═E groups such as [4,5-$(P(E)Ph_2)_2$tz] (E = O(**1a**), S(**1b**), Se(**1c**)) can offer additional coordination sites which can provide unusual structural features and chemical reactivities, as well as enhance the stability of the complexes. Herein, we report the synthesis and structural characterization of $\{\kappa^3$-*N,N′,E*-[4,5-$(P(E)Ph_2)_2(\mu$-tz)]$InMe_2\}_2$ derivatives. Compounds **2**, **3**, and **5** all exhibit the same type of dimeric-like arrangement with a planar In_2N_4 core.

* To whom correspondence should be addressed. Fax: +52 55 56 16 22 17. Tel: +52 55 56 22 44 04. E-mail: monica.moya@correo.unam.mx.
† UNAM.
‡ Georg-August Universität.

(1) (a) Silvestru, C. Drake, J. E. *Coord. Chem. Rev.* **2001**, *223*, 117−216. (b) Hill, M. S.; Hitchcock, P. B.; Karagouni, S. M. A. *J. Organomet. Chem.* **2004**, *689*, 722−730. (c) Power M. B.; Ziller, J. W.; Barron, A. R. *Organometallics* **1993**, *12*, 4908−4916. (d) Aparna, K.; McDonald, R.; Ferguson, M.; Cavell, R. G. *Organometallics* **1999**, *18*, 4241−4243. (e) Ong, C. M.; McKarns, P.; Stephan, D. W. *Organometallics* **1999**, *18*, 4197−4204.

(2) The coordination modes of {[(4,5-$(P(O)Ph_2)_2$tz]Rh(cod)}, {[(4,5-$(P(O)Ph_2)_2$tz]$_3$Mg}[$HNEt_3$], and {[(4,5-$(P(O)Ph_2)_2$tz]$_3$La} have been identified but not fully structurally characterized. See Rheingold, A. L.; Liable-Sands, L. M.; Trofimenko, S. *Angew. Chem., Int. Ed.* **2000**, *39*, 3321−3324.

(3) Rheingold, A. L.; Liable-Sands, L. M.; Trofimenko, S. *Inorg. Chim. Acta*. **2002**, *303*, 38−43.

(4) (a) Rendle, D. F.; Storr, A.; Trotter, J. *Can. J. Chem.* **1975**, *53*, 2944−2954. (b) Rendle, D. F.; Storr, A.; Trotter, J. *Can. J. Chem.* **1975**, *53*, 2930−2943. (c) Rendle, D. F.; Storr, A.; Trotter, J. *J. Chem. Soc., Dalton Trans.* **1973**, 2252−2255. (d) Ward, D. M.; Mann, K. L. V.; Jeffery, J. C.; McCleverty, J. A. *Acta Crystallogr.* **1998**, *C54*, 601−603. (e) Hausen, H. D.; Locke, K.; Weidlein, J. *J. Organomet. Chem.* **1992**, *429*, C27−C32. (f) Zheng, W.; Mösch-Zanetti, N. C.; Roesky, H. W.; Hewitt, M.; Cimpoesu, F.; Schneider, T. R.; Stasch, A.; Prust, J. *Angew. Chem., Int. Ed.* **2000**, *39*, 3099−3102. (g) Zheng, W.; Hohmeister, H.; Mösch-Zanetti, N.; Roesky, H. W.; Noltemeyer, M.; Schmidt, H.-G. *Inorg. Chem.* **2001**, *40*, 2363−2367 and references therein.

10.1021/ic051567p CCC: $33.50
Published on Web 06/03/2006

Experimental Section

General Comments. All reactions and handling of reagents were performed under an atmosphere of dry nitrogen or argon using standard Schlenk techniques or a glovebox where the O_2 and H_2O levels were usually kept bellow 1 ppm. All glassware was oven-dried at 140 °C for at least 24 h, assembled hot, and cooled under high vacuum prior to use. Toluene (Na/benzophenone ketyl), pentane (Na/K/benzophenone ketyl), and tetrahydrofuran (K/benzophenone ketyl) were dried and distilled prior to use. $InMe_3$ (Strem) was used as received, and compounds **1a**−**c** were prepared according to literature procedures.[2,3] Mass spectra were recorded on a Finnigan Mat 8230 instrument, and IR spectra were recorded on a Bio-Rad digilab FTS-7 spectrometer in the 4000−350 cm^{-1} range as Nujol mulls. ^1H (500 MHz) and ^{31}P NMR (202.5 MHz) were recorded on a Bruker Avance 500 NMR spectrometer at −55 or 20 °C, chemical shifts were referenced to TMS (^1H) and H_3PO_4 85% (^{31}P). Elemental analyses were performed by Galbraith Laboratories (Knoxville, TN). Melting points were measured in sealed glass tubes and were not corrected.

Preparation of {κ^3-*N,N′,O*-[4,5-(P(O)Ph$_2$)$_2$(μ-tz)]InMe$_2$}$_2$ (2). A solution of $InMe_3$ (0.16 g, 1 mmol) in hexanes (5 cm^3) was added at ambient temperature to a suspension of **1a** (0.47 g, 1 mmol) in toluene (10 cm^3), gas evolution was observed, during which the solid dissolved completely, and after 10 min a white precipitate was formed. The reaction mixture was filtered, and the solid was washed with toluene (2 × 5 cm^3). The crude product was recrystallized from warm THF (5 cm^3), giving colorless crystals (0.50 g, 81%) mp 250 °C (dec); IR $\tilde{\nu}$(Nujol/cm^{-1}): 2953, 1460, 1376, 1120; ^1H NMR (500 MHz, THF-d_8, 20 °C, TMS) δ 7.98, 7.75 (m, 16H, *o*-Ph−*H*), 7.42−7.17 (m, 24H, *m, p*-Ph−*H*), −0.10 (s, 12H, InC*H*$_3$); ^{31}P NMR (202.5 MHz, THF-d_8, 20 °C, H_3PO_4 85%) δ 32.4 (P═O), 17.7 (P−O(In)); EI-MS (70 eV): *m*/*z* 1211 (M^+ − CH_3, 1), 613 ($M^+/2$ − CH_3, 100). Anal. Calcd for $C_{56}H_{52}In_2N_6P_4O_4$ (1226.60 g·mol^{-1}): C 54.8; H 4.3. Found: C 54.9; H 4.4%.

Preparation of {κ^3-*N,N′,S*-[4,5-(P(S)Ph$_2$)$_2$(μ-tz)]InMe$_2$}$_2$ (3). A similar procedure as that for **2** was used starting from **1b** (0.50 g, 1.0 mmol) and a solution of $InMe_3$ (0.16 g, 1 mmol) in hexanes (5 cm^3), giving pale yellow crystals (0.45 g, 70%) mp 305 °C (dec); IR $\tilde{\nu}$(Nujol/cm^{-1}): 3015, 1438, 1387, 1103; ^1H NMR (500 MHz, THF-d_8, −55 °C, TMS) δ 7.58 (m, 16H, *o*-Ph−*H*), 7.40−7.15 (m, 24H, *m, p*-Ph−*H*), 0.07 (s, 12H, InC*H*$_3$); ^{31}P NMR (202.5 MHz, THF-d_8, −55 °C, H_3PO_4 85%) δ 36.5 (P═S), 30.2 (P−S(In)); EI-MS (70 eV): *m*/*z* 1275 (M^+ − CH_3, 1), 630 ($M^+/2$ − CH_3), 100). Anal. Calcd for $C_{56}H_{52}In_2N_6P_4S_4$ (1290.84 g·mol^{-1}): C 52.1; H 4.1. Found: C 51.8; H 3.9%.

Preparation of {κ^3-*N,N′,Se*-[4,5-(P(Se)Ph$_2$)$_2$(μ-tz)]InMe$_2$}$_2$ (4). A similar procedure as that for **2** was used starting from **1c** (0.59 g, 1.0 mmol) and a solution of $InMe_3$ (0.16 g, 1 mmol) in hexanes (5 cm^3), giving a white crystalline powder (0.51 g, 68%) mp 320 °C (dec); IR $\tilde{\nu}$(Nujol/cm^{-1}): 2923, 1462, 1101, 1377, 687; ^1H NMR (500 MHz, THF-d_8, 20 °C, H_3PO_4 85%): δ 8.13, 7.89 (m, 16H, *o*-Ph−*H*), 7.51, 7.50 (m, 8H, *p*-Ph−*H*), 7.49, 7.44 (m, 16H, *m*-Ph−*H*) 0.19 (s, 12H, InC*H*$_3$). ^{31}P NMR (121.5 MHz, THF-d_8, 20 °C, H_3PO_4 85%) δ 34.3 (P═Se), 11.9 (P−Se(In)); EI-MS (70 eV): *m*/*z* 837 ($C_{21}H_{18}In_2N_6P_3Se_2$, 5), 822 ($C_{20}H_{15}In_2N_6P_3Se_2$, 10), 741 ($M^+$/2, 3), 726 ($M^+/2$ − CH_3, 3), 646 ($M^+/2$ − $SeCH_3$, 100). Anal. Calcd for $C_{56}H_{52}In_2N_6P_4Se_4$ (1478.44 g·mol^{-1}) C 45.5; H 3.6. Found: C 46.7; H 3.8%.

Crystal Data Collection, Structure Solution, and Refinement Details for Compounds 2, 3, and 5·2THF. The diffraction data for the compounds **2**, **3**, and **5**·2THF were measured on a Bruker three-circle diffractometer equipped with a SMART 6000 CCD detector using mirror-monochromated CuK_α radiation (λ = 1.54178 Å). The data for all compounds were collected at 100 K with the PROTEUM[5] program using ϕ- and ω-scans and integrated with the SAINT[5] program. Semiempirical absorption correction from the equivalents was applied (SADABS).[5] The space groups were determined with XPREP[5] program, and the structures were solved by direct methods (SHELXS-97)[6] and refined with all data by full-matrix least-squares methods on F^2 using SHELXL-97.[7]

Scheme 1

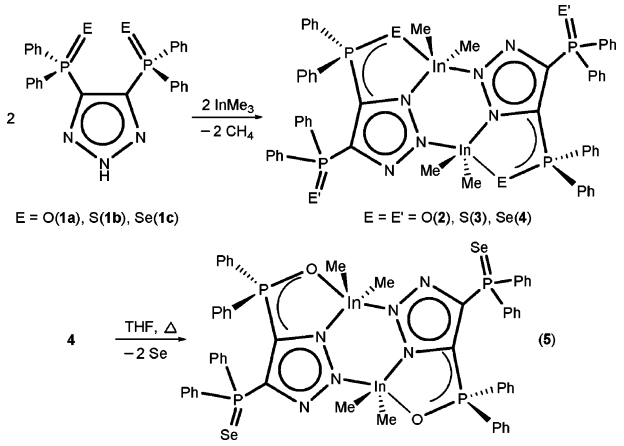

Results and Discusion

Addition of 1 equiv of trimethylindium to the slurry of the free ligand (**1a**−**c**) in toluene resulted in the immediate elimination of methane, during which all the solid was dissolved. After the removal of the toluene under vacuum and washing, the remaining solid with cold hexane, {κ^3-*N,N′,O*-[4,5-(P(O)Ph$_2$)$_2$(μ-tz)]InMe$_2$}$_2$ (**2**), {κ^3-*N,N′,S*-[4,5-(P(S)Ph$_2$)$_2$(μ-tz)]InMe$_2$}$_2$ (**3**), and {κ^3-*N,N′,Se*-[4,5-(P(Se)Ph$_2$)$_2$(μ-tz)]InMe$_2$}$_2$ (**4**) were obtained in good yields (68−81%). In all three cases, the formation of a dinuclear In_2N_4 six-membered ring with coordination of In to one chalcogen atom was observed (Scheme 1).

Compounds **2**−**4** were characterized by analytical and spectroscopic studies, and compounds **2** and **3** were further characterized by X-ray diffraction experiments. The IR spectra of these compounds are all devoid of N−H absorption in the range of 3000−3200 cm^{-1}, and the ^1H NMR spectra (THF-d_8) display the characteristic patterns owing to the deprotonated ligands. The ^{31}P NMR spectra for these complexes at ambient temperature show two broad resonances for **2** (32.4 and 17.7 ppm) and **4** (34.3 and 11.9 ppm). On the other hand, compound **3** exhibited only one broad resonance at 33.5 ppm, although a low-temperature ^{31}P NMR experiment carried out at −55 °C revealed two sharp resonances (36.5 and 30.2 ppm), indicating the presence of a fluxional behavior at ambient temperature. However, low-temperature NMR experiments performed on **2** and **4** resulted merely in the sharpening of their signals. The NMR behavior

(5) *PROTEUM* (v. 1.40), *SAINT* (v. 7.01A), *SADABS* (v. 2004/1), and *XPREP* (v. 2005/1); Bruker Analytical X-ray Instruments, Inc.: Madison, WI.
(6) Sheldrick, G. M. *Acta Crytallogr. Sect. A* **1990**, *46*, 467−473.
(7) Sheldrick, G. M. *SHELXL-97, Program for Crystal Structure Refinement*, Universität Göttingen: Göttingen, Germany, 1997.

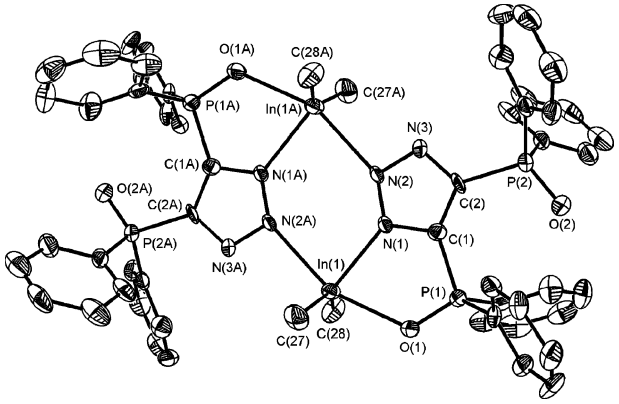

Figure 1. Molecular structure and numbering scheme of molecule 1 of the centrosymmetric dimer **2** (50% probability ellipsoids). All hydrogen atoms are omitted for clarity. For the molecular structure and numbering scheme of molecule 2, see Figure S1 in the Supporting Information.

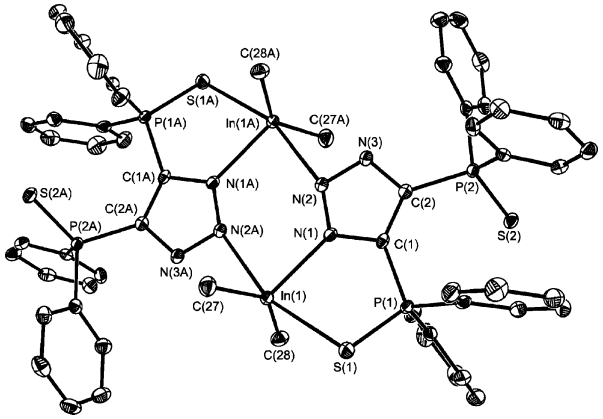

Figure 2. Molecular structure and numbering scheme of the centrosymmetric dimer **3** (50% probability ellipsoids). All hydrogen atoms are omitted for clarity.

of compound **3** contrasts with that in **4** were the strong In−O bonding seems to prevent the ligand exchange process taking place at ambient temperature. Whereas, in the case of **4**, the larger size of the selenium atom (compared to that of the sulfur atom in **3**) seems to contribute to a higher energetic barrier for the same type of exchange process and is therefore slow in the NMR time scale at ambient temperature.

Electron impact (EI) spectrometry revealed peaks at *m*/*z* 1211 and 1275 corresponding to the $(M^+ - CH_3)$ fragments for **2** and **3**, respectively. Compound **4** exhibits a $(M^+/2)$ peak at *m*/*z* 741 along with higher fragments at *m*/*z* 822 ($C_{20}H_{15}{}^{115}In_2N_6P_3{}^{80}Se_2$) and 837 ($C_{21}H_{18}{}^{115}In_2N_6P_3{}^{80}Se_2$) which reveal its dimeric nature.

In an attempt to grow X-ray-quality crystals of **4** from hot THF, precipitation of red selenium was observed. Further structural analysis of the product revealed the replacement of the selenium atom in the P−Se(In) moiety by an oxygen atom, leading to the formation of a mixed-chalcogen complex (**5**) (Scheme 1). To gain further insight on this chalcogen exchange process, we performed controlled hydrolysis and oxidation experiments on **1c** and **4**.[8] Unfortunately, none of these reactions led to the formation of the mixed-chalcogen species, and thus far, we have not been able to reproduce the synthesis of **5**.

Structural Description. Colorless X-ray-quality crystals of **2**, **3**, and **5**·2THF were obtained by slowly cooling their saturated THF solutions from 65 °C to ambient temperature.

Compounds **2**, **3**, and **5** crystallize in a triclinic space group $P\bar{1}$ with two independent halves of the molecule (**2**) (Figure 1), one-half of the molecule (**3**) (Figure 2), and one-half of the molecule solvated by one THF molecule (**5**) (Figure 3) in the asymmetric unit, respectively. The crystal data and refinement details for all three structures are tabulated in Table 1, and selected bond lengths and angles complexes **2**, **3**, and **5** are listed in Table 2.

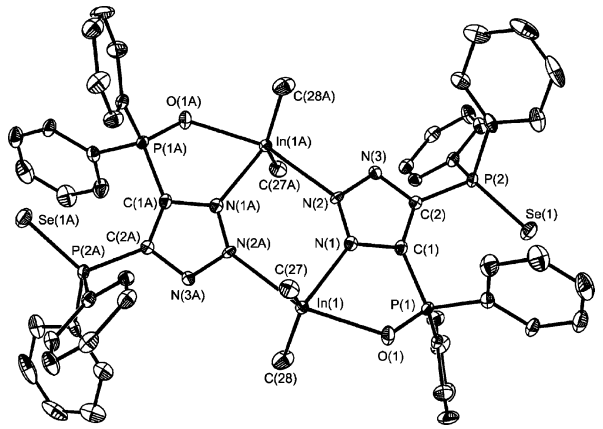

Figure 3. Molecular structure and numbering scheme of the centrosymmetric dimer **5**·2 THF (50% probability ellipsoids). All hydrogen atoms and the solvating THF molecules are omitted for clarity.

The central $C_4In_2N_6O_2P_4$ core in both independent molecules in **2** exhibits an almost planar arrangement with a mean deviation of 0.019 and 0.042 Å. Whereas, for compound **5**, the mean deviation of these atoms is 0.100 Å, and finally, the planarity disappears in **3** (mean deviation is 0.223 Å).

The degree of delocalization of the electron densities in these structures is also reflected by the deviation of chalcogen atom of the terminal P═E moiety from the central plane mentioned above. This deviation is 0.371 and 0.485 Å for **2**, 0.482 Å for **5**, and 1.885 Å for **3**, respectively. In all three complexes, the In atom has a distorted trigonal-bipyramidal environment with the methyl groups and N(1) from the triazole ring occupying the equatorial plane (sum of the angles: 359.8° and 360.0° (**2**), 359.1° (**3**), and 360° (**5**)). The axial positions are occupied by a chalcogen atom and the N(2) belonging to the second triazole ring of the dimer, in which case significantly bent angles (157.3° and 155.7° (**2**), 161.8° (**3**), and 158.4° (**5**)) are observed.

The equatorial In−N(1) bond (2.297 and 2.302 (**2**), 2.280 (**3**), and 2.312 Å (**5**)) is common for the five- and six-

(8) Addition of stoichiometric amounts of H_2O to a boiling solution of **4** in THF resulted merely in the isolation of **1c**; the same result was observed by bubbling air through the solution at ambient temperature and at 65 °C. In a similar manner, addition of stoichiometric amounts of H_2O to a boiling solution of **1c** in THF did not lead to the chalcogen exchange, even when dry HCl was added as a catalyst. Although, oxidation of **1c** was successful with H_2O_2, it led to the rapid deposition of red selenium and formation of an inseparable mixture of oxidation compounds. For a similar chalcogen exchange reaction involving P═E groups, see Hong, F.-E.; Chang, Y.-C.; Chang, R.-E.; Chen, S.-C.; Ko, B.-T. *Organometallics* **2002**, *21*, 961−967.

Table 1. Crystal Data and Structure Refinement for Compounds **2**, **3**, and **5**·2THF

compound	**2**	**3**	**5**·2THF
formula	$C_{56}H_{52}In_2N_6O_4P_4$	$C_{56}H_{52}In_2N_6P_4S_4$	$C_{64}H_{68}In_2N_6O_4P_4Se_2$
fw	1226.56	1290.80	1496.68
cryst syst	triclinic	triclinic	triclinic
space group	$P\bar{1}$	$P\bar{1}$	$P\bar{1}$
a, Å	12.845(2)	11.431(3)	8.266(2)
b, Å	15.074(3)	11.503(3)	12.569(3)
c, Å	16.198(3)	11.741(3)	16.847(3)
α, deg	67.03(3)	86.24(3)	74.98(3)
β, deg	70.30(3)	85.73(3)	79.71(3)
γ, deg	73.19(3)	63.71(3)	72.69(3)
V, Å^3	2673 (1)	1379(1)	1604(1)
Z	2	1	1
$\rho_{calcld.}$, g·cm^{-3}	1.524	1.554	1.549
μ, mm^{-1}	8.442	9.534	8.389
F(000)	1240	652	752
cryst size, mm^3	0.11 × 0.02 × 0.01	0.15 × 0.04 × 0.01	0.15 × 0.04 × 0.02
θ range for data collection, deg	3.06 to 56.92	3.78 to 57.89	2.73 to 57.81
no. of reflns collected	18 883	13 247	12 903
no. of indep. reflns (R_{int})	6911 (0.0462)	3659 (0.0221)	4224 (0.0350)
no. of data/restraints/params	6911/0/653	3659/0/328	4224/0/372
GOF on F^2	1.022	1.058	1.046
R1,[a] wR2[b] ($I > 2\sigma(I)$)	0.0569, 0.1380	0.0171, 0.0444	0.0320, 0.0701
R1,[a] wR2[b] (all data)	0.0826, 0.1546	0.0175, 0.0459	0.0422, 0.0737
largest diff. peak/hole, e·Å^{-3}	3.933/−0.994	0.338/−0.304	1.594/ −0.486

[a] $R1 = \sum||F_o| - |F_c||/\sum|F_o|$. [b] $wR2 = [\sum w(F_o^2 - F_c^2)^2/\sum w(F_o^2)^2]^{1/2}$.

Table 2. Selected Bond Distances (Å) and Angles (deg) for Compounds **2**, **3**, and **5**

		Compound **2**	
molecule a			
In(1)−O(1)	2.318(5)	N(1)−In(1)−N(2A)	82.6(2)
In(1)−N(1)	2.297(6)	C(27)−In(1)−C(28)	140.5(4)
In(1)−N(2A)	2.465(6)	N(1)−In(1)−C(27)	108.1(3)
In(1)−C(27)	2.145(9)	N(1)−In(1)−C(28)	111.2(3)
In(1)−C(28)	2.132(8)	N(1)−In(1)−O(1)	74.8(2)
N(1)−N(2)	1.328(9)	N(2A)−In(1)−O(1)	157.3(2)
N(2)−N(3)	1.333(8)	P(1)−O(1)−In(1)	122.8(3)
P(1)−O(1)	1.505(5)		
P(2)−O(2)	1.480(6)		
molecule b			
In(2)−O(3)	2.319(5)	N(4)−In(2)−N(5A)	81.7(2)
In(2)−N(4)	2.302(6)	C(55)−In(2)−C(56)	135.8(3)
In(2)−N(5A)	2.495(6)	N(4)−In(2)−C(55)	112.4(3)
In(2)−C(55)	2.158(8)	N(4)−In(2)−C(56)	111.8(3)
In(2)−C(56)	2.186(7)	N(4)−In(2)−O(3)	74.0(2)
N(4)−N(5)	1.333(8)	N(5A)−In(2)−O(3)	155.7(2)
N(5)−N(6)	1.334(9)	P(3)−O(3)−In(2)	123.2(3)
P(3)−O(3)	1.504(6)		
P(4)−O(4)	1.484(5)		
		Compound **3**	
In(1)−S(1)	2.780(1)	N(1)−In(1)−N(2A)	83.5(1)
In(1)−N(1)	2.280(2)	C(27)−In(1)−C(28)	141.6(1)
In(1)−N(2A)	2.583(2)	N(1)−In(1)−C(27)	109.9(1)
In(1)−C(27)	2.140(2)	N(1)−In(1)−C(28)	107.6(1)
In(1)−C(28)	2.136(2)	N(1)−In(1)−S(1)	78.3(1)
N(1)−N(2)	1.339(2)	N(2A)−In(1)−S(1)	161.8(1)
N(2)−N(3)	1.327(3)	P(1)−S(1)−In(1)	96.7(4)
P(1)−S(1)	1.986(1)		
P(2)−S(2)	1.948(1)		
		Compound **5**	
In(1)−O(1)	2.336(3)	N(1)−In(1)−N(2A)	84.7(1)
In(1)−N(1)	2.311(4)	C(27)−In(1)−C(28)	142.5(2)
In(1)−N(2A)	2.499(6)	N(1)−In(1)−C(27)	107.2(2)
In(1)−C(27)	2.142(5)	N(1)−In(1)−C(28)	110.3(2)
In(1)−C(28)	2.152(5)	N(1)−In(1)−O(1)	73.8(1)
N(1)−N(2)	1.345(5)	N(2A)−In(1)−O(1)	158.4(1)
N(2)−N(3)	1.331(5)	P(1)−O(1)−In(1)	120.5(2)
P(1)−O(1)	1.515(3)		
P(2)−Se(1)	2.090(2)		

membered rings (InNCPE and In_2N_4) and is shorter than the In−N(2) in the axial position (2.465 and 2.495 (**2**), 2.583 (**3**), and 2.499 Å (**5**)) belonging to the In_2N_4 core. All the In−N bond lengths are significantly longer than those found in the related $(InMe_2)_2(\mu\text{-pz})_2$ [4e] (av 2.209) and $(InCl_2)_2(\mu\text{-3-(2-pyridyl)-1H-pz})_2(DMF)_2$ [4d] (av 2.209). The In−Me bond lengths are similar in all three compounds (av 2.155 (**2**), av 2.138 (**3**), and av 2.147 Å (**5**)) and are comparable to those in $(InMe_2)_2(\mu\text{-pz})_2$ [4e] (av 2.144 Å). Furthermore, these bond lengths belong to the shorter ones reported in the CCDC database (see In−Me bond length histogram from CCDC in the Supporting Information, Figure S2).

The average N−N distances within the triazole ring for all three compounds are almost identical (1.332 (**2**), 1.333 (**3**), and 1.338 Å (**5**)). Thus, the differences in the In−In separations (4.90 and 4.96 (**2**), 4.93 (**3**), and 4.88 Å (**5**)) are mainly due to the variation of the In−N bond lengths and inner angles of the In_2N_4 ring system. The sums for these inner angles (the theoretical value for a planar, six-membered ring cores is 720°) are 719.8° and 720.0° (**2**), 711.8° (**3**), and 716.2° (**5**), respectively. The In−O bond lengths in **2** (2.318 and 2.319 Å) and **5** (2.336 Å) have similar values and when taking into account the difference of the covalent radii for the oxygen (0.68 Å) and sulfur atoms (1.02 Å) these are comparable also to the In−S bond length in **3** (2.780 Å).[9] (For more details about the selected bond lengths for **2**, **3**, and **5** see Table 2)

These In−E bond lengths are the longest ones observed so far for any In−E−P-moiety-containing system. The P−O(In) bond lengths (1.505 and 1.504 Å for **2**; 1.515 Å for **5**) are slightly longer than those of the terminal P═O (1.480 and 1.482 Å for **2**), thus confirming the high degree of electron delocalization in **2** and **5**. Similar effects can be also found in **3** for the P−S(In) (1.986 Å) and P═S bonds (1.948 Å), but in this case, the difference is higher (for the

(9) For a table of covalent atomic radii, see the web page of the Cambridge Structural Database: http://www.ccdc.cam.ac.uk/products/csd/radii/.

histograms of (P)E−In and P−E terminal bond lengths see Figure S2 in the Supporting Information).

Conclusion

In summary, we explored the bonding properties of the multidentate ligands [4,5-($P(E)Ph_2)_2$tz] (E = O, S, Se) with indium. The results show that this ligand is capable of achieving unconventional phosphoranyl complexes which contain free P═E reaction sites that can be utilized for further transformation or complexation reactions. Although the formation mechanism of **5** remains unclear, further research on this issue is currently underway.

Acknowledgment. M.M.-C. thanks the DGAPA-UNAM (PAPIIT Grant No. IN105203) for financial support. V.J. thanks the UNAM for his postdoctoral fellowship. This paper is dedicated to Professor Raymundo Cea-Olivares on the occasion of his 55th birthday.

Supporting Information Available: Figure S1 featuring molecule 2 of compound **2**; histograms from CCDC; and X-ray data (CIF) for **2**, **3**, and **5**. This material is available free of charge via the Internet at http://pubs.acs.org.

IC051567P